Journal of Materials Chemistry C

Accepted Manuscript

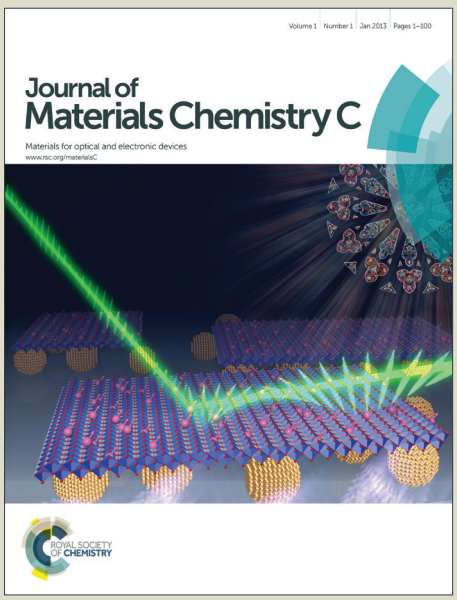

ROYAL SOCIETY OF CHEMISTRY

www.rsc.org/materialsC

Late Stage Crystallization and Healing During Spin-Coating Enhance Carrier Transport in Small-Molecule Organic Semiconductors

Kang Wei Chou[†], Hadayat Ullah Khan[†], Muhammad R. Niazi[†], Buyi Yan[†], Ruipeng Li[†], Marcia M. Payne[ξ], John E. Anthony[ξ], Detlef-M. Smilgies[‡], and Aram Amassian[†,]*

[†] Physical Sciences and Engineering Division, Solar and Photovoltaic Engineering Research Center, King Abdullah University of Science and Technology (KAUST), Thuwal 23955-6900, Saudi Arabia

[ξ]Department of Chemistry, University of Kentucky, Lexington, Kentucky 40506, United States

[‡]Cornell High Energy Synchrotron Source, Cornell University, Ithaca, New York 14853, United States

*Email: aram.amassian@kaust.edu.sa

Keywords: organic thin-film transistors, small-molecule, spin casting, time-resolved grazing incidence wide-angle x-ray scattering.

ABSTRACT

Spin coating is currently the most widely used solution processing method in organic electronics. Here, we report, for the first time, a direct investigation of the formation process of the small-molecule organic semiconductor (OSC) 6,13-bis(triisopropylsilylethynyl) (TIPS)-pentacene during spin-coating in the context of an organic thin film transistor (OTFT) application. The solution thinning and thin film formation were monitored *in situ* by optical reflectometry and grazing incidence wide angle X-ray scattering, respectively, both of which were performed during spin-coating. We find that OSC thin film formation is akin to a quenching process, marked by a deposition rate of ~100 nm/s, nearly three orders of magnitude faster than drop-casting. This is then followed by a more gradual crystallization and healing step which depends upon the spin speed. We associate this to further crystallization and healing of defects by residency of the residual solvent trapped inside the kinetically trapped film. The residency time of the trapped solvent is extended to several seconds by slowing the rotational speed of the substrate and is credited with improving the carrier mobility by nearly two orders of magnitude. Based on this insight, we deliberately slow down the solvent evaporation further and demonstrate improved carrier mobility by an additional

order of magnitude. These results demonstrate how spin-coating conditions can be used as a handle over the crystallinity of organic semiconductors otherwise quenched during initial formation only to recrystallize and heal during extended interaction with the trapped solvent.

INTRODUCTION

In recent years, solution-processed small-molecule organic thin-film transistors (OTFTs) have achieved field-effect mobilities well in excess of 1 cm^2 $V^{-1}s^{-1}$, with some reports of field effect mobilities above 10 cm^2 $V^{-1}s^{-1}$.[1-5] Such transistor mobilities increasingly surpass those of the best OTFTs prepared via vacuum evaporation and also the performance of hydrogenated amorphous silicon devices by nearly an order of magnitude.[6,7] The characteristics of solution-processed OTFTs can vary dramatically depending on the solution processing conditions, especially in the case of small-molecule organic semiconductors, since thin film nucleation and crystallization are highly sensitive to solution drying kinetics.[8] Understanding the link between processing conditions and thin film formation and crystallization processes is therefore critical to the successful solution-processing of high performance organic electronic devices.[9-11]

Although new deposition methods like blade coating, solution shearing, inkjet printing and spray coating are making important advances in the processing of organic semiconductor thin films,[1,3,12,13] spin coating remains one of the most widely used lab-based solution-processing methods both for material screening and device optimization. Uniform, thin, smooth and continuous films are achieved by depositing a drop of solution and subsequently spreading/ejecting and drying it at high rotational speed. During drop casting, the crystallization of the active layer is dictated by the vapor pressure of the solvent and temperature of the solution, and the time scale of crystallization may range from seconds to hours, making it subject to substrate-induced dewetting.[8,14,15] During spin casting, on the other hand, this time may be reduced to the sub-second range by virtue of the rotational speed, which ejects excess solution and causes accelerated drying of the solution.[16,17] Spin casting is thus a highly non-equilibrium process, potentially quenching the solid film formation process and greatly impacting the development of the microstructure.

Current studies of process-structure-performance relationships in organic electronics rely mostly on post-deposition characterization of thin films. Structural studies of this type provide important insight into the final structure of films. However, the understanding of the mechanism of thin film formation in relation to the processing conditions, such as spin speed, remains undetermined. Clearly, the ability to monitor the solution to solid phase transformation during the spin coating process is critical for the understanding of the process-structure-performance relationships in spin-coated OTFTs. Time-resolved laser reflectance measurements have already been successfully deployed during the spin coating process to study the evolution of the in-plane phase separation during film formation and to evaluate the spatially averaged drying rates of polymer blended films.[18,19] Ebbens et al. also developed a stroboscopic imaging technique to record optical micrographs of the film formation and phase separation during the spin coating process.[20,21] This technique allowed the reconstruction of the height profile with a precision comparable to atomic force microscopy (AFM). We have recently demonstrated the use of in situ time-resolved UV-visible absorption measurements during spin-coating of polymer semiconductors, revealing the state of aggregation of the polymer semiconductor in the bulk solution as well as the importance of managing the kinetics of solution drying.[17] The above-mentioned techniques provide valuable morphological information of polymer blends in the micrometer range and insight into photophysical aggregation, but fail to provide information on the crystallization behavior of small-molecule thin films, where complex processes, such as transient polymorphism, may occur at the early stages of growth.[22,23]

Time-resolved x-ray reflectivity and scattering techniques have been successfully applied in the past to the study of vacuum-deposited small-molecule thin films by both thermal and hyperthermal processes on bare and chemically treated inorganic and organic surfaces,[23-29] and to investigate the effects of solvent vapor annealing of small-molecule thin films.[14,30] More recently, x-ray scattering has been used to investigate solution processing of small-molecule thin films, including drop-casting and blade-coating of small-molecule thin films for OTFTs[8,31] and spin-coating of polymer:fullerene[16] and molecule:fullerene[22,32] bulk heterojunction organic photovoltaics.

Here, we report the direct investigation of the crystallization behavior of a small-molecule organic semiconductor prepared by spin coating and its influence on charge carrier mobility in OTFTs by performing in situ and real-time grazing incidence wide angle x-ray scattering (GIWAXS) during the spin coating process. The functionalized pentacene, 6,13-bis(triisopropylsilylethynyl) (TIPS) pentacene (see also Figure 1a), was chosen for this study, as it is a widely studied soluble organic small-molecule semiconductor capable of achieving carrier mobilities well above 1 cm^2 $V^{-1}s^{-1}$.[1,4] The film formation was investigated for different spin speeds, ranging between 1000 and 2000 rpm, a rather small range selected to demonstrate the importance of small variations in processing conditions on the kinetics of crystallization. We find the crystallization process to be marked first by a fast step function and followed by a slower crystallization step. To our surprise, we find the fast formation step to be relatively insensitive to the processing conditions investigated despite significant differences in the solvent evaporation rate just prior to the onset of nucleation, whereas the duration of the late stage crystallization is highly dependent upon the selected spin speed. The change of the evaporation rate and the associated slow crystallization step are shown to strongly affect the carrier mobility by nearly two orders of magnitude. These results reveal new insight into the crystallization process during spin coating of small-molecule organic semiconductors and highlight the important role of solvent evaporation kinetics and residency time in mediating the microstructural outcome of spin coating. We have further used these insights to fabricate OTFTs using very slow spin speed (300 rpm) and demonstrate devices yielding a another order of magnitude improvement in carrier mobility. These improvements in carrier transport are reminiscent of the beneficial effects of solvent vapor annealing at the right dose on the performance of small-molecule OTFTs.[14]

EXPERIMENTAL DETAILS

Sample description. The acene-based small-molecule semiconductor 6,13-bis(triisopropylsilylethynyl) (TIPS) pentacene (Figure 3a), first described by Anthony and co-workers,[32] was dissolved in toluene (1 wt.%) in normal ambient conditions and stirred overnight at room temperature. All depositions were performed at room temperature on pre-cut silicon oxide wafers. The wafers were cleaned by consecutively ultrasonicating in soapy de-ionized (DI) water, DI water, toluene, acetone and isopropanol for 20 minutes each. As the substrate needs to be hydrophilic in order to achieve high surface coverage of the TIPS-

pentacene film, the sonication was followed by UV ozone treatment for 10 minutes. All solution and sample preparations for the x-ray characterization and device fabrication were performed in air.

Characterization techniques. The spin coating of TIPS-pentacene was studied at different spin speeds (1000 rpm, 1250 rpm, 1500 rpm, 1750 rpm and 2000 rpm). Polarized optical micrographs were taken in transmission mode through crossed polarizers using a Nikon Eclipse LV100POL Polarizing Microscope. Scattering experiments were performed at the D1 station at the Cornell High Energy Synchrotron Source (CHESS, Ithaca, NY) and a Pilatus 100k detector was used with a framing rate of 10 Hz and exposure time of 0.09 seconds. The setup is shown in Figure 3a. The hard x-ray beam had a wavelength of 1.1688 Å and a width of about 0.1 mm. The beam was incident at an angle of 0.15° with respect to the sample plane, which is above the critical angle of the organic semiconductor and below the critical angle of silicon. Silver behenate was used for calibration. The penetration depth for toluene at 10.6 keV is 2.66 mm. For an incidence angle of 0.15°, the maximum thickness in order for the x-rays to reach the substrate is about 3.5 μm. The feasibility of in situ time-resolved GIWAXS during drop-casting and spin-casting was recently demonstrated.[8,16] The intensity evolution of the (001) Bragg sheet and satellite peak during the spin coating process were investigated. The final thickness of the films was evaluated using a Dektak Profilometer. A small scratch was applied to remove the film locally from the sample surface and measure the film thickness. In situ time-resolved optical reflectometry measurements were performed using a F20-UVX spectrometer (Filmetrics, Inc.) equipped with a tungsten halogen and a deuterium light source (Filmetrics, Inc.) over the wavelength range from 400 nm to 1700 nm. Most measurements were performed with an integration time of 0.15 s per reflection spectrum. The solution thickness was extracted using a fast Fourier transform (FFT) algorithm in the thick film regime (> 1 μm) and a coarse model fit based on the transfer matrix formalism over the wavelength range 800-1700 nm for thinner films (< 1 μm). High-speed optical microscopy measurements were performed at KAUST on a Nikon LV100 microscope and recorded by a Photron SA-3 CMOS camera mounted on the microscope. The images were recorded at a speed of 3600 frames per second.

Device fabrication. A highly doped n-type silicon wafer (100) with thermally oxidized 300 nm thick SiO_2 was used as bottom gate and gate dielectric for top contact organic field-effect transistor (OFET) fabrication. Prior to deposition of the organic semiconductor, the substrates were also cleaned by

consecutive ultrasonication of the substrate in soapy DI water, pure DI water, toluene, acetone and isopropanol for 20 minutes each. All substrates were blown dry with N_2 and followed with UV ozone treatment for 10 minutes to form a hydrophilic surface. Solutions of TIPS-pentacene were prepared in toluene (1 wt.%) as described above. A pipette was used to drop 80 µl of TIPS-pentacene solution onto the Si/SiO_2 substrates and the solution was immediately spin coated in air. Gold source and drain electrodes were deposited by evaporation through a shadow mask with a channel width (W) of 500 µm and length (L) of 50 µm. All electrical measurements were performed using a Keithley 4200 Semiconductor Characterization System under N_2 atmosphere inside a nitrogen-filled glove box.

RESULTS AND DISCUSSION

A 50 µl drop of the OSC solution was cast on a clean substrate and immediately spin coated for a duration of 50 seconds. Five different spinning speeds were used (1000, 1250, 1500, 1750 and 2000 rpm) to prepare the various thin films. A series of high speed optical micrographs of the first second of spin-coating experiment are shown in Figures 1a, 1b and 1c, revealing that the process is initially dominated by a liquid ejection regime. In situ time-resolved optical reflectometry measurements were performed for all five spinning conditions and the time-evolution of solution thickness are summarized in Figure 1d. The thickness evolution appears to be independent of spin speed at early times as it is dominated by solution ejection, but transitions after ~1 second to an evaporation-dominated regime which depends upon rotation speed. From the linear thinning regime below ~5 µm wet film, we determine the rate of evaporation to range between ~1.6 and ~4 µm/s, for spin speeds ranging between 1000 and 2000 rpm, respectively. The solution drying time is therefore a strong function of spin speed and ranges between ~2.4 s (2000 rpm) and ~5.4 s (1000 rpm).

An overview of the static GIWAXS patterns right after the spin coating process (exposure time of 1 second) is presented in Figure 2, together with static polarized optical microscopy (POM) images showing the polycrystalline appearance of the thin films. The thickness of the dry films was measured by profilometry and is found to decrease with increasing spin speeds from 66 nm to 37 nm, respectively. This is due to more ejection of the bulk solution during the early stages of spin coating (see inset of Figure 1d).

The POM images clearly show an increase in lateral feature size and a tendency to form spherulitic shaped domains at lower spin speeds. At high spin speeds, the film is composed of a uniform distribution of small domains. The scattering images in Figure 2 were background subtracted with a scattering pattern obtained without the film. The high intensity in the q_z direction represents the (001) Bragg sheet associated to lamellar stacking (peak at q_z around 0.4 $Å^{-1}$), and indicates a highly lamellar ordered thin film well-known to have an "edge-on" orientation with brickwork packing motif and two-dimensional π-π stacking that favors charge-transport in the plane of the semiconductor thin film (Figure 3a).[33] The (001) Bragg sheet of the TIPS-pentacene crystallites have a d-spacing between 1.6 – 1.7 nm (the detailed values are summarized in the supplementary information). The small satellite peak at an azimuthal angle of about 65º represents the (001)' peak in the <111> orientation and indicates the formation of a mixed polycrystalline texture. Further quantitative comparison of degree of crystallinity on the basis of diffraction peak intensity is difficult given the significant differences in physical thickness. Using the Scherrer equation,[34] an out-of-plane correlation length can be derived from the full width at half maximum (FWHM) along the q_z direction. The correlation length has a decreasing trend for increasing spin speeds from 16.3 nm down to 12.5 nm, respectively. The physical thickness is nearly 3-4 times greater than the crystalline thickness estimated by the Scherrer formula, suggesting the film thickness is made up of several lamellar crystallites of TIPS-pentacene. This ratio is similar to drop-cast films of TIPS-pentacene of similar thickness prepared from toluene.[8] The azimuthal spread is an indicator for the in-plane mosaicity of the film and was evaluated at the different spin speeds for the (001) and (001)' peaks, respectively. Here, a decrease can be found in the width for increasing spin speeds from 14.8º to 11.0º for the (001) peak, and from 16.0º to 13.3º for the (001)' peak, indicating a slightly improved lamellar texture in films cast at increasing spinning speed.

The time evolution of the crystallization process was investigated in situ using time-resolved GIWAXS during spin coating (Figure 3a) and by monitoring and plotting the integrated intensity of the (001) and (001)' reflections with respect to the spin coating time with 0 second corresponding to the moment spinning starts.[16] In Figure 3b, we show the time-evolution of the (001) normalized intensity for TIPS-pentacene films prepared at all spinning speeds. As no differences could be found in the crystallization kinetics of (001) and (001)' reflections, we conclude TIPS-pentacene crystallizes in these two orientations

simultaneously. We have therefore limited the data representation in Figure 3b to the evolution of the (001) Bragg sheet intensity, as this had a far better signal-to-noise-ratio than (001)'. Not surprisingly, the onset of crystallization (nucleation) is a strong function of the spin speed, decreasing by nearly a factor of two, as was previously suggested by optical measurements of solution thinning (Figure 1). As the in situ optical reflectometry and in situ GIWAXS measurements were performed separately, a direct one-to-one quantitative comparison of the onset of crystallization with respect to solution thickness or concentration cannot be established with a high degree of reliability and has therefore not been performed.

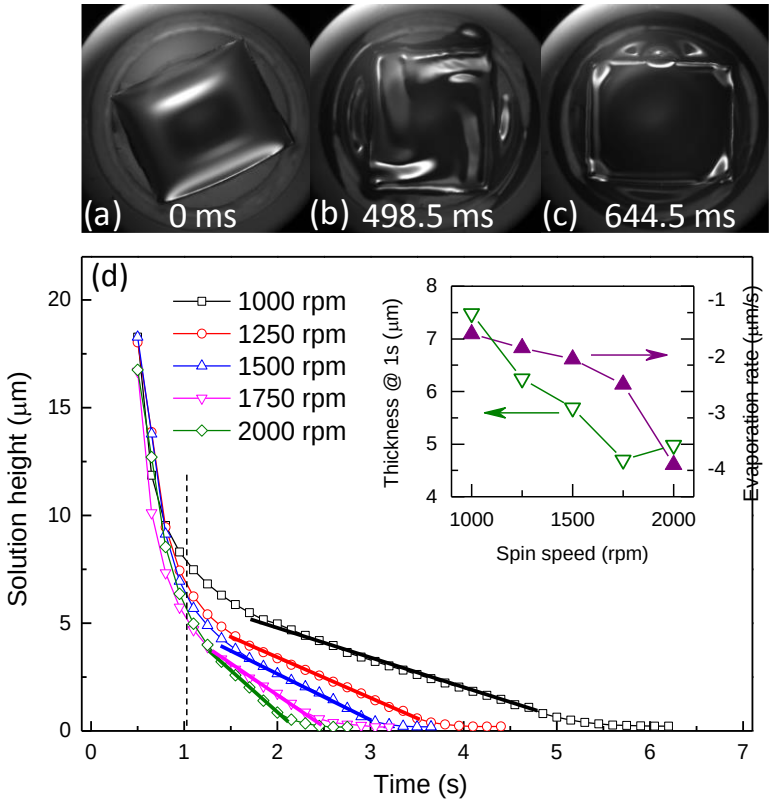

Figure 1: (a, b, c) High speed optical micrographs of the spin-coating process (1000 rpm) revealing bulk liquid ejection well within the first half second of the spin-coating process. (d) In situ thickness evolution obtained from optical reflectometry measurements performed during spin-coating, revealing the thinning behavior of TIPS-pentacene in toluene solution spin-cast at different spinning speeds. Spin-coating is characterized by rapid hydrodynamic thinning at first, followed by evaporation-dominated thinning. The inset shows the thickness of the solution after 1 second of spin coating as well as the rate of evaporation versus spin speed, as determined from the slope of solution height versus time in the evaporative regime.

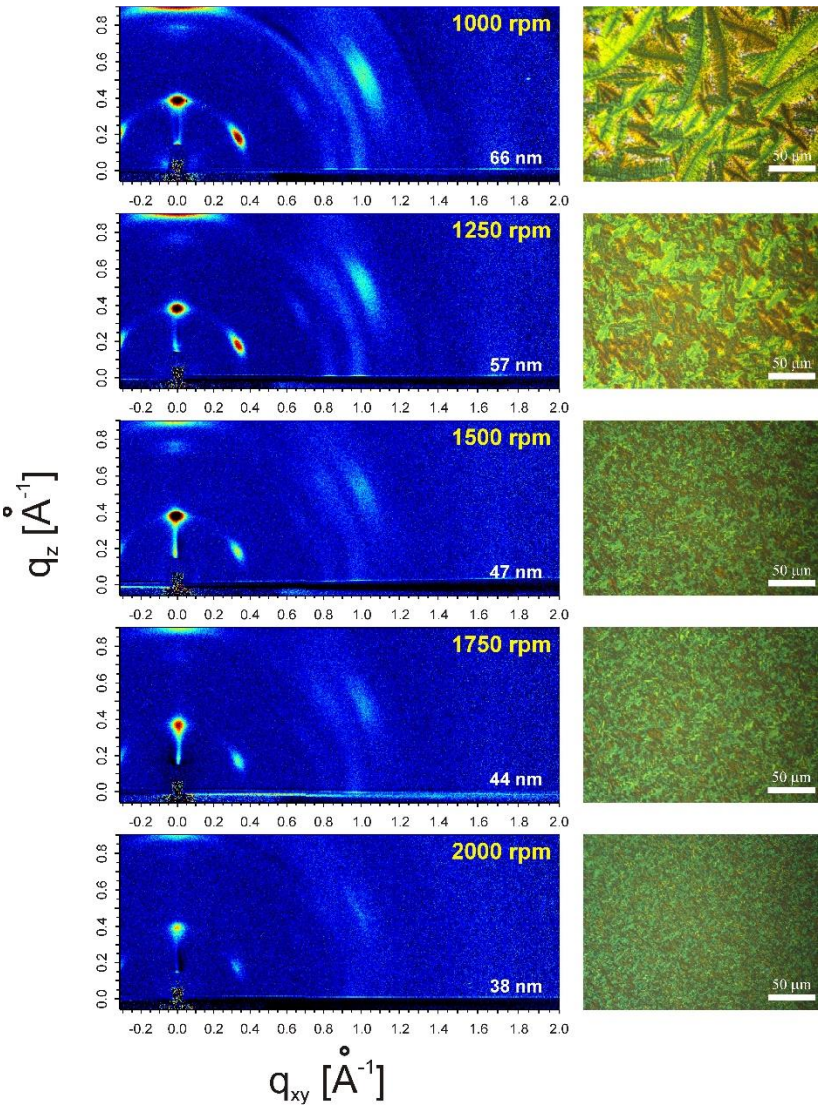

Figure 2: The left column summarizes the GIWAXS patterns for TIPS pentacene thin-films, as cast by spin coating at different spinning speeds. The corresponding POM images are shown in the right column. The (001) ordering peak is at a q_z around 0.4 Å^{-1}. The thickness of the films was measured using a profilometer.

In Figure 4a, only the lowest and highest spinning speeds are considered and an abrupt increase can be observed in the normalized peak intensity just a few seconds after the onset of spin coating (highlighted in yellow). The increase indicates a rapid crystallization process over a sub-second timescale. Following this sharp rise, the curves are marked by a slower, more gradual increase (green guide line added), followed by

a plateau a few seconds later indicating completion of the crystallization process. Remarkably, the duration of the rapid crystallization process is independent of the spin speed, whereas the duration of the slow crystallization process is very much spinning speed-dependent. The timeline of the crystallization process is graphically summarized in Figure 4b for all spin speeds and the exact values can be found in the Supplementary Information (Table S2). The duration of the rapid crystallization process (the width of the yellow area as seen in Figure 4a and 4b varies between 0.12 sec and 0.28 sec) does not appear to show any obvious dependency on the spinning speed. The onset of fast crystallization and the duration of the slow crystallization process, on the other hand, do show clear dependencies. Logically, at lower spin speeds, less solution is ejected during acceleration (as indicated by the final film thicknesses) and overall the solvent evaporates more slowly, leaving a little more solvent in the drying film, most likely at grain boundaries. The amount of residual solvent cannot be quantified easily, but it is most certainly present as it is the only plausible explanation as to why lamellar crystallization still proceeds for several seconds after the rapid crystallization step instead of quenching rapidly. The ejection of less solvent at slow speed and the slower evaporation rate of the solution explains both the longer delay before the onset of fast crystallization at lower spin speeds (wider black area in Figure 4b) and a slower crystallization after the fast jump of more than 8 seconds at 1000 rpm (green area in Figure 4b). This slowing down of the kinetics of the second crystallization step at lower spin speeds eventually allows the film to form larger crystalline domains as observed in the POM images in Figure 2, while at high spin speeds we observe the nucleation and growth of much smaller domains.

Bottom gate, top contact organic thin film transistors (OTFTs) were fabricated under the same conditions as the *in situ* GIWAXS experiments. The average saturation hole mobility, the threshold voltage and the current on/off ratio were extracted from the transfer curves and summarized in the supporting information (Figure S4). The carrier mobility shows a strong dependence with the spin speed, increasing by nearly two orders of magnitude with decreasing spin speed from 5×10^{-4} cm^2 $V^{-1}s^{-1}$ (2000 rpm) to 2.2×10^{-2} cm^2 $V^{-1}s^{-1}$ (1000 rpm). However, as noted earlier, the duration of the rapid crystallization step does not change with the spin speed and therefore cannot account for the significant variations of OTFT performance. Instead, it appears as though the second stage of crystallization influences the microstructure and the carrier mobility

much more. In Figure 5, we plotted the carrier mobility with respect to the total crystallization time, namely the sum of the durations of both the rapid and the slow crystallization processes. The plot shows a clear correlation between the carrier mobility of the TIPS-pentacene thin films and the total duration of the crystallization process. It is well known that charge transport, for instance in organic thin film transistors, correlates well with the crystalline order in small-molecule semiconductor thin films, on the condition that said film is also continuous and the semiconductor is π-stacked in the plane of the semiconductor-dielectric interface.[33] As the films appear to cover the substrate in its entirety, it appears that the improved microstructure is entirely responsible for the improvement in device performance, as seen previously.[11,36] The thickness of thin films differs, but it is not expected to directly influence the carrier transport, because all films are in excess of 35 nm thickness and appear to show no pinholes or any evidence of de-wetting.[14,37]

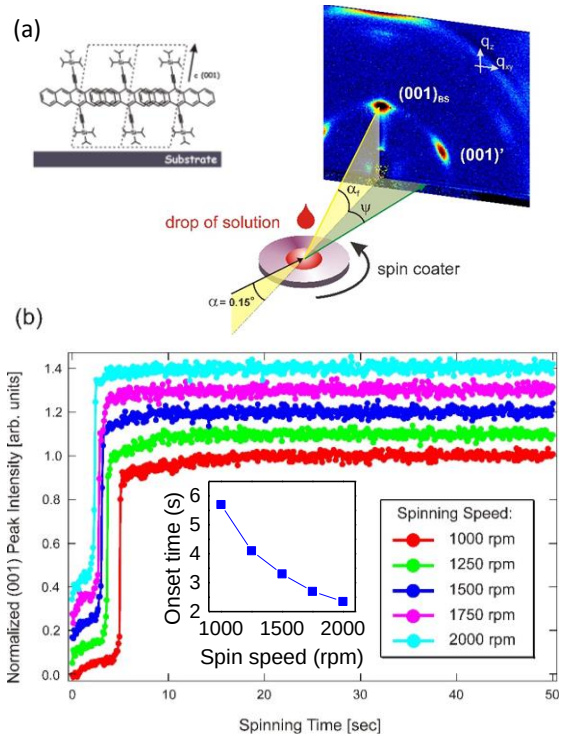

Figure 3: (a) Schematic of the in situ GIWAXS setup allowing time-resolved measurements, during the spin coating process, of the (001) Bragg sheet and the (001)' Bragg peak at 65° off normal. The inset shows the orientation of the TIPS pentacene crystallites with respect to the substrate. (b) Time-evolution of the (001) Bragg sheet intensity (area under the curve) for all spin speeds. Inset shows the onset of crystallization with respect to the spin speed.

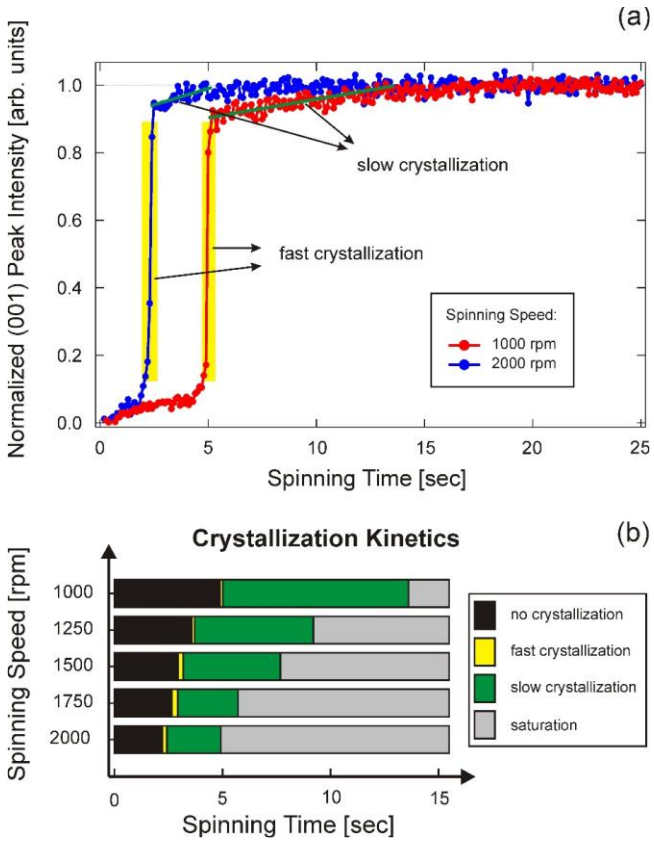

Figure 4: Panel (a) shows curves of the normalized (001) peak intensity in function of the spinning time during the spin coating process, for the lowest and highest spinning speed (1000 and 2000 rpm, respectively). The regions of interest (fast and slow crystallization) are marked. The duration of the different processes is summarized in panel (b) for all spinning speeds, as can be derived from the curves in the upper panel.

In a prior investigation of the role of solvent vapor annealing of spin cast TIPS-pentacene thin films from a toluene-based solution, a quartz crystal microbalance with dissipation (QCM-D) was used to detect both the uptake of solvent vapor molecules and the resulting viscoelastic properties of the film and solvent.[14] For very small doses of solvent vapor, the solvent molecules were found to adsorb without forming a liquid phase and further crystallization was promoted without causing the film to dewet. This resulted in improvements of the carrier mobility by up to 2 orders of magnitude. The device performance degraded quite dramatically, however, as soon as the solvent vapor molecules formed into the liquid phase on the surface of the film, highlighting the delicate balancing role that a solvent plays in achieving highly

crystalline organic semiconductor thin films. Unlike in the current study, the apparent size of crystalline domains did not increase by solvent vapor annealing; only the lamellar texture and crystallinity improved. This suggests there may be differences in the nucleation density of TIPS pentacene with increasing spin speed despite apparently exhibiting identical crystallization kinetics in the first regime of nucleation and growth, as observed by the in situ GIWAXS measurements.

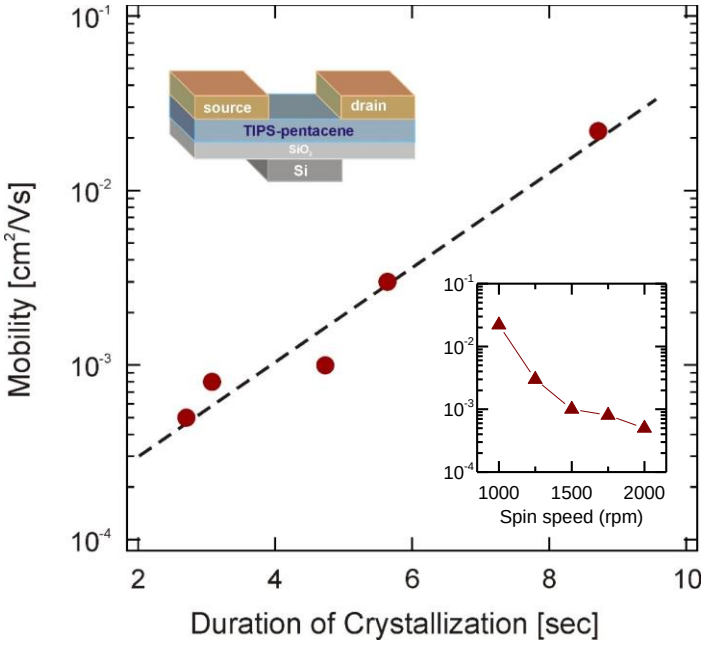

Figure 5: Linear dependency of the hole mobility versus the duration of crystallization (width of the green bars in Figure 4b, representing the slow crystallization time) for TIPS pentacene OFETs prepared with different spinning speeds. The inset shows the carrier mobility with respect to the spin coating speed.

In the spin-coating experiments reported in this study, the spinning speed modulates the evaporation rate of the solution, as shown by the in situ time-resolved optical reflection measurements (Figure 1). These measurements revealed that solution thinning is dominated by evaporation for solution thicknesses below 5 μm and that evaporation is significantly slowed down by decreasing the spin speed. This decrease is seen both in the drying rate of the bulk solution (1 – 5 μm) and in the final stage of the drying process (< 1 μm). Case in point, the time it takes for the last micron of the solution to reach the steady (dry) thickness

increases from ~0.6 s (2000 rpm) to ~0.8 s (1500 rpm) and up to ~1.35 s (1000 rpm). This hints that the solvent may reside for even an extended period in the forming film, as strongly suggested by the in situ GIWAXS measurements (Figure 4), and which is likely to promote significant coarsening of the crystallites. The rate of evaporation prior to nucleation and growth of the TIPS pentacene crystallites may promote a different nucleation density, with higher nucleation density occurring for faster drying solutions and a slower nucleation density occurring in case of slow-drying solutions, as suggested by the POM micrographs of the final thin films. However, we have also shown that the spin speed strongly modulates the residence time of trapped solvent in the film and thus promote further crystallization activity well after the initial film formation.

As the slow evaporation rate combined with minute amounts of solvent trapped in the film appear to have a dramatic effect on the crystallization behavior, we attempt to further slow the evaporation process and extend the residency time of the residual solvent by further slowing down the spin speed. We have fabricated OTFTs using conditions of very slow spin coating speed (300 rpm), for which the device characteristics and performance metrics are shown in Figure 6 and Table 1, respectively. The resulting OTFTs perform remarkably well, with an average (peak) carrier mobility of 0.28 (0.47) $cm^2 V^{-1}s^{-1}$, which is a full order of magnitude higher than what was achieved at 1000 rpm. This also surpasses what previously has been achieved by spin coating followed by solvent vapor annealing[8] and approaches the performance of OTFTs typically achievable by drop-casting.

The observations made in this study are consistent with a recent report in which high boiling point solvent additives, such as diphenyl ether and chloronaphthalene, when used in appropriate amounts, resulted in larger crystallites and in better performing devices.[38,39] Indeed, the role of high boiling point solvent additives has been investigated extensively in the context of bulk heterojunction organic photovoltaics (OPV) and has been correlated to the further ripening of the blend after the rapid film formation stage is completed.[40-43] In the case of solution processable small-molecule OPVs, *in situ* GIWAXS measurements performed during spin-coating demonstrated that the right amount of diiodooctane in the solution promotes molecular reorganization of the donor and leads to the formation of a thermodynamically stable polymorph

of the donor, which does not otherwise form without the use of the additive.[22] This phase transformation is responsible for the high power conversion efficiency in the resulting solar cells. The results of the current study nevertheless demonstrate that some of the benefits of solvent additives can be achieved by extending the residency of the processing solvent in the film during and shortly after the thin film formation and crystallization stage.

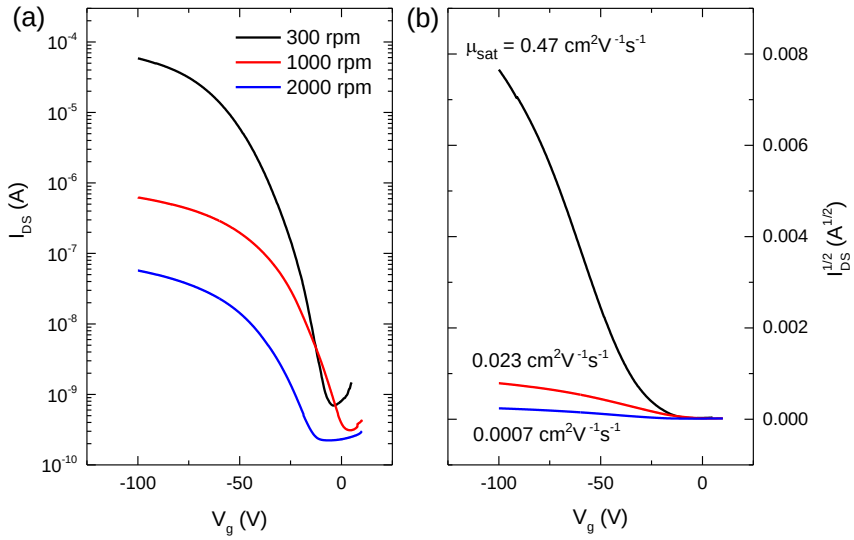

Figure 6: Current-voltage sweeps (a) I_{DS}-V_G and (b) $I_{DS}^{1/2}$-VG for organic thin film transistors fabricated by spin coating a TIPS-pentacene solution at 300 rpm, 1000 rpm and 2000 rpm.

Table 1: Summary of the average device characteristics for organic thin film transistors fabricated by spin coating a TIPS-pentacene solution at a very slow speed of 300 rpm.

Spin Speed	Avg. Mobility [cm^2 V^{-1}s^{-1}]	Std deviation [cm^2 V^{-1}s^{-1}]	V_{th} [V]	I_{on}/I_{off}
300 rpm	0.28	±0.14	-25 (±4)	10^5
1000 rpm	0.021	±0.002	-2 (±2)	$4\cdot10^3$
2000 rpm	0.0005	±0.0002	-16 (±2)	$3\cdot10^2$

CONCLUSIONS

Research in the growth and structural evolution of spin-cast organic semiconductor thin films has until recently been limited to post-deposition characterization and has thus resulted in limited insight into the mechanisms of thin film formation. The main cause for this shortcoming has been the absence of in situ characterization tools to investigate common processes, such as spin-coating. Here, we have shown that time-resolved GIWAXS can be employed to study the crystallization during the spin-coating process of organic semiconductors, such as TIPS-pentacene. We provide relevant crystallization data with a time resolution of 100 ms, which makes it possible to follow the kinetics of crystallization and detect two distinct stages of crystallization characterized by their different kinetics. A linear dependency is found between the hole mobility and the total crystallization time, which includes the period of time required for drying of the residual solvent trapped in the thin film. The best transistor characteristics are observed in conditions, which avoided rapid quenching of the crystallization, instead letting the residual solvent evaporate and promote further grain growth. The spin-cast films at lower spinning speeds resulted in the formation of large spherulitic domains as opposed to the much smaller domains formed at higher spinning speeds. This methodology can easily be translated to a wide variety of systems requiring or relying upon spin coating to achieve films with controlled crystallization and/or phase separation in areas such as electronics, optoelectronics, photovoltaics, thermoelectrics and energy storage.

ASSOCIATED CONTENT

Supporting information

Radially and azimuthally integrated curves and characteristic dimensions of TIPS pentacene deposited at different spinning speeds. Integrated intensity of the (001) peak in the <001> orientation and <111> orientation during the spin coating of the TIPS pentacene solution at the different spinning speeds. Characteristic times and durations of crystallization. Average saturation hole mobility, threshold voltage and current on/off ratio of OTFT devices.

AUTHOR INFORMATION

Corresponding author

*Email: aram.amassian@kaust.edu.sa

ACKNOWLEDGEMENTS

The authors thank the Fréchet group at UC Berkeley for providing access to a fume hood during synchrotron experiments and for help with profilometry measurements and the Thoroddsen group at KAUST for assistance with high speed optical imaging of the spin-coating process. We'd like to thank Eunhee Lim of the Advanced Light Source for technical assistance. Research reported in this publication was supported by the King Abdullah University of Science and Technology (KAUST) and by KAUST's Office of Competitive Research Funds under award number FIC/2010/04. The authors acknowledge use of the D1 beam line at the Cornell High Energy Synchrotron Source supported by the National Science Foundation and NIH-NIGMS via NSF grant DMR-0225180.

REFERENCES

(1) Diao, Y.; Tee, B. C-K.; Giri, G.; Xu, J.; Kim, D. H.; Becerril, H. A.; Stoltenberg, R. M.; Lee, T. H.; Xue, G.; Mannsfeld, S. C. B.; Bao, Z. Solution coating of large-area organic semiconductor thin films with aligned single-crystalline domains. *Nat. Mat.* **2013**, 12, 665–671.

(2) Smith, J.; Zhang, W.; Sougrat, R.; Zhao, K.; Li, R.; Cha, D.; Amassian, A.; Heeney, M.; McCulloch, I.; Anthopoulos, T. D. Solution-Processed Small Molecule-Polymer Blend Organic Thin-Film Transistors with Hole Mobility Greater than 5 cm^2/Vs. *Adv. Mat.* **2012**, 24, 2441–2446.

(3) Minemawari, H.; Yamada, T.; Matsui, H.; Tsutsumi, J.; Haas, S.; Chiba, R.; Kumai, R.; Hasegawa, T. Inkjet printing of single-crystal films. *Nature* **2011**, 475, 364-367.

(4) Giri, G.; Verploegen, E.; Mannsfeld, S. C. B.; Atahan-Evrenk, S.; Kim, D. H.; Lee, S. Y.; Becerril, H. A.; Aspuru-Guzik, A.; Toney, M. F.; Bao, Z. Tuning charge transport in solution-sheared organic semiconductors using lattice strain. *Nature* **2011**, 480, 504-508.

(5) Yu, L.; Li, X.; Smith, J.; Tierney, S.; Sweeney, R.; Kjellander, B. K. C.; Gelinck, G. H.; Anthopoulos, T. D.; Stingelin, N. Solution-processed small molecule transistors with low operating voltages and high grain-boundary anisotropy. *J. Mater. Chem.* **2012**, 22, 9458–9461.

(6) Sze, S. M. Semiconductor Devices: Physics and Technology, John Wiley and Sons, New York, NJ 2002.

(7) Dimitrakopoulos, C. D.; Malenfant, P. R. L. Organic Thin Film Transistors for Large Area Electronics. *Adv. Mater.* **2002**, 14, 99-117.

(8) Li, R.; Khan, H. U.; Payne, M. M.; Smilgies, D.-M.; Anthony, J. E.; Amassian. A. Heterogeneous Nucleation Promotes Carrier Transport in Solution-Processed Organic Field-Effect Transistors. *Adv. Funct. Mater.* **2013**, 23, 291-297.

(9) Dickey, K. C.; Anthony, J. E.; Loo, Y. L. Improving Organic Thin-Film Transistor Performance through Solvent-Vapor Annealing of Solution-Processable Triethylsilylethynyl Anthradithiophene. *Adv. Mater.* **2006**, 18, 1721-1726.

(10) Loo, Y. L. Solution-processable organic semiconductors for thin-film transistors: Opportunities for chemical engineers. *AIChE Journal* **2007**, 53, 1066-1074.

(11) Loo, Y. L.; McCulloch, I. Progress and challenges in commercialization of organic electronics. *MRS Bull.* **2008**, 33, 653-662.

(12) Mei, Y.; Loth, M. A.; Payne, M.; Zhang, W.; Smith, J.; Day, C. S.; Parkin, S. R.; Heeney, M.; McCulloch, I.; Anthopoulos, T. D.; Anthony, J. E.; Jurchescu, O. D. High Mobility Field-Effect Transistors with Versatile Processing from a Small-Molecule Organic Semiconductor. *Adv. Mat.* **2013**, 25, 4352–4357.

(13) Giri, G.; Li, R.; Smilgies, D.-M.; Li, E. Q.; Diao, Y.; Lenn, K. M.; Chiu, M.; Lin, D. W.; Allen, R.; Reinspach, J.; Mannsfeld, S. C. B.; Thoroddsen, S. T.; Clancy, P.; Bao, Z., Amassian, A. One-dimensional self-confinement promotes polymorph selection in large-area organic semiconductor thin films. *Nature Comm.* 2014, 5, 3573.

(14) Khan, H. U.; Li, R.; Ren, Y.; Chen, L.; Payne, M. M.; Bhansali, U. S.; Smilgies, D.-M.; Anthony, J. E.; Amassian, A. Solvent Vapor Annealing in the Molecular Regime Drastically Improves Carrier Transport in Small-Molecule Thin-Film Transistors. *ACS Appl. Mater. Interfaces* **2013**, 5, 2325–2330.

(15) Treat, N. D.; Nekuda Malik, J. A.; Reid, O.; Yu, L.; Shuttle, C. G.; Rumbles, G.; Hawker, C. J.; Chabinyc, M. L.; Smith, P.; Stingelin, N. Microstructure formation in molecular and polymer semiconductors assisted by nucleation agents. *Nature Mater.* **2013**, 12, 628-633.

(16) Chou, K. W.; Yan, B.; Li, R.; Li, E. Q.; Zhao, K.; Anjum, D. H.; Alvarez, S.; Gassaway, R.; Biocca, A.; Thoroddsen, S. T.; Hexemer, A.; Amassian, A. Spin-Cast Bulk Heterojunction Solar Cells: A Dynamical Investigation. *Adv. Mat.* **2013**, 25, 1923–1929.

(17) Abdelsamie, M.; Zhao, K.; Niazi, M. R.; Chou, K. W.; Amassian, A. In situ UV-visible absorption during spin-coating of organic semiconductors: a new probe for organic electronics and photovoltaics. *J. Mater. Chem. C* **2014**, 2, 3373–3381.

(18) Jukes, P. C.; Heriot, S. Y.; Sharp, J. S.; Jones, R. A. L. Time-Resolved Light Scattering Studies of Phase Separation in Thin Film Semiconducting Polymer Blends during Spin-Coating. *Macromolecules* **2005**, 38, 2030–2032.

(19) Mokarian-Tabari, P.; Geoghegan, M.; Howse, J. R.; Heriot, S. Y.; Thompson, R. L.; Jones, R. A. L. Quantitative evaluation of evaporation rate during spin-coating of polymer blend films: Control of film structure through defined-atmosphere solvent-casting. *Eur. Phys. J. E* **2010**, 33, 283– 289.

(20) Ebbens, S.; Hodgkinson, R.; Parnell, A. J.; Dunbar, A.; Martin, S. J.; Topham, P. D.; Clarke, N.; Howse, J. R. InSitu Imaging and Height Reconstruction of Phase Separation Processes in Polymer Blends during Spin Coating. *ACS Nano* **2011**, 5, 5124-5131.

(21) Toolan, D. T. W.; Pullan. N.; Harvey, M. J.; Topham, P. D.; Howse, J. R. In Situ Studies of Phase Separation and Crystallization Directed by Marangoni Instabilities During Spin-Coating. *Adv. Mat.* **2013**, 25, 7033–7037**.**

(22) Perez, L. A.; Chou, K. W.; Love, J. A.; van der Poll, T. S.; Smilgies, D.-M.; Nguyen, T.-Q.; Kramer, E. J.; Amassian, A.; Bazan, G. C. Solvent Additive Effects on Small Molecule Crystallization in Bulk Heterojunction Solar Cells Probed During Spin Casting. *Adv. Mater.* **2013**, 25, 6380–6384.

(23) Kowarik, S.; Gerlach, A.; Sellner, S.; Schreiber, F.; Cavalcanti, L.; Konovalov, O. Real-Time Observation of Structural and Orientational Transitions during Growth of Organic Thin Films. *Phys. Rev. Lett.* **2006**, 96, 125504.

(24) Mayer, A. C.; Ruiz, R.; Headrick, R. L.; Kazimirov, A.; Malliaras, G. G. Early stages of pentacene film growth on silicon oxide. *Organic Electronics* **2004**, 5, 257–263.

(25) Moulin, J.-F.; Dinelli, F.; Massi, M.; Albonetti, C.; Kshirsagar, R.; Biscarini, F. In situ X-ray synchrotron study of organic semiconductor ultra-thin films growth. *Nucl. Instr. and Meth. in Phys. Res. B* **2006**, 246, 122-126.

(26) Hong, S.; Amassian, A.; Woll, A. R; Bhargava, S.; Ferguson, J. D.; Malliaras, G. G.; Brock, J. D.; Engstrom, J. R. Real time monitoring of pentacene growth on SiO2 from a supersonic source. *Appl. Phys. Lett.* **2008**, 92, 253304.

(27) Amassian, A.; Desai, T. V.; Kowarik, S.; Hong, S.; Woll, A. R.; Malliaras, G. G.; Schreiber, F.; Engstrom, J. R. Coverage dependent adsorption dynamics in hyperthermal organic thin film growth. *J. Chem. Phys.* **2009**, 130, 124701.

(28) Amassian, A.; Pozdin, V. A.; Desai, T. V.; Hong, S.; Woll, A. R.; Ferguson, J. D.; Brock, J. D.; Malliaras, G. G.; Engstrom, J. R. Post-deposition reorganization of pentacene films deposited on low-energy surfaces. *J. Mater. Chem.* **2009**, 19, 5580-5592.

(29) Desai, T. V.; Woll, A. R.; Schreiber, F.; Engstrom, J. R. Nucleation and Growth of Perfluoropentacene on Self-Assembled Monolayers: Significant Changes in Island Density and Shape with Surface Termination. *J. Phys. Chem. C* **2010**, 114, 20120-20129.

(30) Amassian, A.; Pozdin, V. A.; Li, R.; Smilgies, D.-M.; Malliaras, G. G. Solvent vapor annealing of an insoluble molecular semiconductor. *J. Mater. Chem.* **2010**, 20 2623-2629.

(31) Smilgies, D.-M.; Li, R.; Giri, G.; Chou, K. W.; Diao, Y.; Bao, Z.; Amassian, A. Look fast: Crystallization of conjugated molecules during solution shearing probed in-situ and in real time by X-ray scattering. *Phys. Status Solidi RRL* **2013**, 7, 177-179.

(32) Liu, F.; Gu, Y.; Wang, C.; Zhao, W.; Chen, D.; Briseno, A. L.; Russell, T. P. Efficient Polymer Solar Cells Based on a Low Bandgap Semi-crystalline DPP Polymer-PCBM Blends *Adv. Mater.* **2012**, 24, 3947-3951.

(33) Anthony, J. E.; Brooks, J. S.; Eaton, D. L.; Parkin, S. R. Functionalized Pentacene: Improved Electronic Properties from Control of Solid-State Order. *J. Am. Chem. Soc.* **2001**, 123, 9482-9483.

(34) Scherrer, P. Bestimmung der Größe und der inneren Struktur von Kolloidteilchen mittels Röntgenstrahlen. *Nachrichten von der Gesellschaft der Wissenschaften zu Göttingen* **1918**, 26, 98-100.

(35) Yang, S. Y.; Shin, K.; Kim, S. H.; Jeon, H.; Kang, J. H.; Yang, H.; Park, C. E. Enhanced Electrical Percolation Due to Interconnection of Three-Dimensional Pentacene Islands in Thin Films on Low Surface Energy Polyimide Gate Dielectrics. *J. Phys. Chem. B* **2006**, 110, 20302–20307.

(36) Shin, S.-I.; Kwon, J.-H.; Kang, H.; Ju, B.-K. Solution-processed 6,13-bis(triisopropylsilylethynyl) (TIPS) pentacene thin-film transistors with a polymer dielectric on a flexible substrate. *Semicond. Sci. Technol.* **2008**, 23, 085009.

(37) Ruiz, R.; Papadimitratos, A.; Mayer, A. C.; Malliaras, G. G. Thickness Dependence of Mobility in Pentacene Thin-Film Transistors. *Adv. Mater.* **2005**, 17, 1795–1798.

(38) Chae, G. J.; Jeong, S.-H.; Baek, J. H.; Walker, B.; Song, C. K.; Seo, J. H. Improved performance in TIPS-pentacene field effect transistors using solvent additives. *J. Mater. Chem. C* **2013**, 1, 4216-4221.

(39) Liu, F.; Wang, C.; Baral, J.; Zhao, W.; Zhang, L.; Watkins, J. J.; Briseno, A. L.; Russell, T. P. Relating Chemical Structure to Device Performance via Morphology Control in Diketopyrrolopyrrole-Based Low Band Gap Polymers. *J. Am. Chem. Soc.* **2013**, 35, 19248.

(40) Peet, J.; Kim, J. Y.; Coates, N. E.; Ma, W. L.; Moses, D.; Heeger, A. J.; Bazan. G. C. Efficiency enhancement in low-bandgap polymer solar cells by processing with alkane dithiols. *Nat. Mater.* **2007**, 6, 497-500.

(41) Lee, J. K.; Ma, W. L.; Brabec, C. J.; Yuen, J.; Moon, J. S.; Kim, J. Y.; Lee, K.; Bazan, G. C.; Heeger, A. J. Processing additives for improved efficiency from bulk heterojunction solar cells. *J. Am. Chem. Soc.* **2008**, 130, 3619-3623.

(42) Chen, H.-Y.; Yang, H. C.; Yang, G. W.; Sista, S.; Zadoyan, R. B.; Li, G.; Yang, Y. Fast-Grown Interpenetrating Network in Poly(3-hexylthiophene): Methanofullerenes Solar Cells Processed with Additive. *J. Phys. Chem. C* **2009**, 113, 7946-7953.

(43) He, Z.; Zhong, C.; Huang, X.; Wong, W.-Y.; Wu, H.; Chen, L.; Su, S.; Cao, Y. Simultaneous Enhancement of Open-Circuit Voltage, Short-Circuit Current Density, and Fill Factor in Polymer Solar Cells. *Adv. Mater.* **2011**, 23, 4636–4643.

Table of Contents Graphic

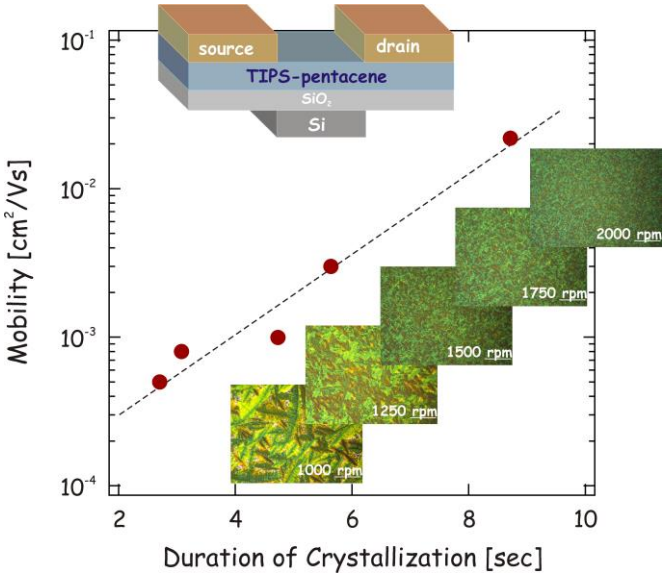

Spin-coating of TIPS-pentacene is examined in-situ to reveal that residual solvent can heal structural defects and dramatically increase carrier mobility.